ACS APPLIED MATERIALS & INTERFACES

Research Article

www.acsami.org

Sulfhydryl-Modified Fe_3O_4@SiO_2 Core/Shell Nanocomposite: Synthesis and Toxicity Assessment in Vitro

Xueyi Guo,*[,†] Fangfang Mao,[†] Weijia Wang,[†] Ying Yang,[†] and Zhiming Bai[‡]

[†]School of Metallurgy and Environment, Central South University, Changsha 410083, PR China

[‡]Haikou Municipal People's Hospital, Haikou 570208, PR China

ABSTRACT: The objectives of this study are to prepare sulfhydryl-modified Fe_3O_4@SiO_2 core/shell magnetic nanocomposites, assess their toxicity in vitro, and explore their potential application in the biomedical fields. Fe_3O_4 nanoparticles synthesized by facile solvothermal method were coated with SiO_2 via the Stöber method and further modified by the *meso*-2,3-dimercaptosuccinic acid (DMSA) to prepare Fe_3O_4@SiO_2@DMSA nanoparticles. The morphology, structure, functional groups, surface charge, and magnetic susceptibility of the nanoparticles were characterized by transmission electron microscopy, X-ray diffraction, Fourier transform infrared spectrometry, X-ray photoelectron spectroscopy, zeta potential analysis, dynamic laser scattering, and vibrating sample magnetometer. Cytotoxicity tests and hemolysis assay were also carried out. Experimental results show that the toxicity of sulfhydryl-modified Fe_3O_4@SiO_2 core/shell nanoparticles in mouse fibroblast (L-929) cell lines is between grade 0 and grade 1, and the material lacks hemolytic activity, indicating good biocompatibility of this Fe_3O_4@SiO_2@DMSA nanocomposite, which is suitable for further application in biochemical fields.

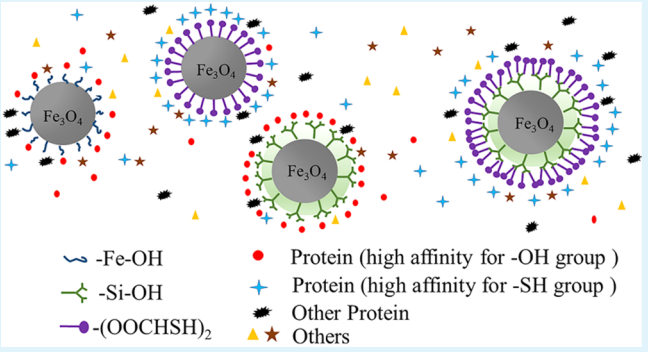

KEYWORDS: *Fe_3O_4 nanoparticles, Fe_3O_4@SiO_2 nanocomposites, core−shell structure, sulfhydryl modification, toxicity assessment, biocompatibility*

INTRODUCTION

It is well-known that magnetic nanoparticles show unique physical and chemical properties and have been extensively applied in biomedical fields, such as biosensing,[1] magnetic resonance imaging (MRI),[2] labeling and sorting of cells,[3] tissue-specific releasing of therapeutic agents,[4] and separation of biochemical products.[5] Previous studies revealed that Fe_3O_4 magnetic nanoparticles (MNPs) could penetrate into cells and accumulate in mitochondria, vesicles, phagosomes, and lysosomes.[6,7] Surface functionalization of Fe_3O_4 can help to stabilize the nanoparticles in biological media and prevent their uptake by the Resovist.[6] It is also shown that coating of MNPs with functional groups can efficiently improve their internalization in many cell types.[8,9] Many materials such as carbon,[10,11] noble metals,[12] metal oxides,[13] and chitosan[14] are considered to be good alternatives for the surface modification of iron oxide. Among these, silica offers the combined benefits of the required properties of biocompatibility, biodegradability, and low toxicity.[15] Also, the availability of −OH moieties can provide binding sites for other organic molecules, which may further extend biological applications.[16]

A lot of efforts have been made to prepare functionalized Fe_3O_4@SiO_2 with noble metals, polymer, and folic acid for biomedical uses.[17−19] Specifically, many reports have given prominence to surface functionalization with sulfhydryl by which the chemical properties such as dispersibility and compatibility of Fe_3O_4@SiO_2 nanocomposites can be improved dramatically.[20−22] Dimercaptosuccinic acid (DMSA)-functionalized Fe_3O_4 recently attracted considerable attention as a new class of highly dispersible biocompatible material.[23−25] Fe_3O_4@DMSA nanoparticles are proposed for numerous biomedical applications such as electrochemical sensors, cell labeling, and drug delivery because of the special properties of sulfhydryl groups that makes them preferable in biological applications.[23−25] However, there is limited information about a facile synthetic route to prepare Fe_3O_4@SiO_2@DMSA nanoparticles, and few investigations concerned on their biocompatibility.

In this paper, we report a simple and effective way to synthesize the sulfhydryl-modified Fe_3O_4@SiO_2 core/shell nanocomposites. Fe_3O_4 nanoparticles synthesized by the facile solvothermal method were coated with SiO_2 via the Stöber method and further modified by DMSA to prepare the target Fe_3O_4@SiO_2@DMSA nanocomposites. In addition, the biocompatibility of sulfhydryl-modified Fe_3O_4@SiO_2 nanocomposites was investigated in this work by cytotoxicity tests and hemolysis assay with a wide range of particle concentration. Moreover, the comparative analysis of biocompatibility of naked Fe_3O_4 MNPs, DMSA-modified Fe_3O_4 MNPs (Fe_3O_4@

Received: May 5, 2015
Accepted: June 17, 2015
Published: June 17, 2015

DOI: 10.1021/acsami.5b03873
ACS Appl. Mater. Interfaces 2015, 7, 14983−14991

Scheme 1. Functional Groups and Protein Absorption on the Surface of Magnetic Nanoparticles in Biological Media

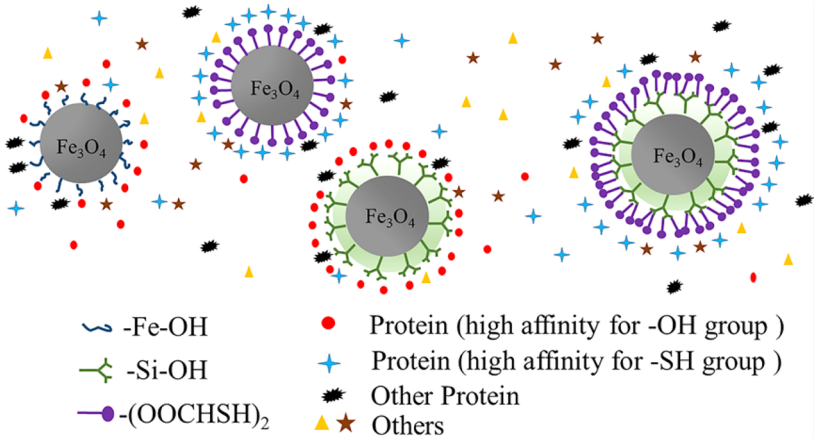

DMSA), SiO_2-coated Fe_3O_4 MNPs (Fe_3O_4@SiO_2), and Fe_3O_4@SiO_2@DMSA nanocomposites were also carried out in the study. The protein adsorption on the surface of magnetic nanoparticles can be dramatically influenced because of the different surface functionalities, which forms the so-called protein corona (Scheme1).

EXPERIMENTAL SECTION

Materials. L-929 mouse fibroblast cells were provided by the China Infrastructure of Cell Line Resources (Shanghai, China). Dimethyl sulfoxide (DMSO), aqueous ammonia (25%−28%), tetraethyl orthosilicate (TEOS), *meso*-2,3-dimercaptosuccinic acid (DMSA), 5, 5-dithiobis(2-nitrobenzoic acid) (DTNB), and ethanol were purchased from Aladdin Industrial Corporation (Shanghai, China) and were analytical-reagent-grade. Dulbecco's modified Eagle's medium (DMEM), fetal bovine serum (FBS), phosphate-buffered saline (PBS), penicillin, and streptomycin were obtained from Dawnrays (Guangdong, China). Toluene, 3-(4,5-dimethylthiazol-2-yl)-2, 5-diphenyltetrazolium bromide (MTT), and fresh human blood were provided by Haikou People's Hospital (Hainan, China). Water used in all experiments was purified using a Milli-Q Plus 185 water purification system (Millipore, Bedford, MA).

Synthesis of Fe_3O_4@SiO_2 Core−Shell MNPs. The Fe_3O_4 magnetic nanoparticles were supplied by Research Institute of Resource Recycling, Central South University (Changsha, China). To synthesize the Fe_3O_4@SiO_2 nanocomposite, 100 mg of the as-prepared hydrophilic Fe_3O_4 MNPs were suspended in ethanol (150 mL) under sonication for 40 min. Aqueous ammonia (3 mL) and deionized water (47 mL) were added in sequence to the suspension, and the mixture (ethanol−water−ammonia solution, 75.0/23.5/1.5 v/v/v %) was sonicated for 40 min. Then, 0.6 mL of TEOS was added slowly under mild continuous stirring at room temperature for another 8 h. The silica-coated nanocomposites were isolated by magnetic separation and were washed with ethanol several times. The final product was collected and dried at 60 °C under vacuum.

Preparation of Sulfhydryl-Modified Fe_3O_4@SiO_2 MNPs. A 100 mg portion of Fe_3O_4@SiO_2 MNPs were dispersed in 10 mL of toluene under sonication for 30 min, and then 10 mL of DMSO and 250 mg of DMSA were added to the solution. The mixture was stirred for 12 h. The final products were collected by magnetic separation, washed with ethanol and deionized water several times, and dried at 60 °C under vacuum.

Characterization. The size and morphology of Fe_3O_4@SiO_2@DMSA MNPs were confirmed by TEM using a TECNAI G2 60-300 analytical electron microscope operating at 200 kV. X-ray diffraction (XRD) data were acquired on a Rigaku D/max X-ray diffractometer (Cu Kα). Fourier transform infrared (FTIR) spectra were determined on a NICOLET 6700 FTIR spectrometer over a potassium bromide pellet. Colloidal characterization was performed by dynamic light scattering (DLS), and zeta potentials of the nanoparticles at a different pH values were measured by Malvern Zetasizer Nano-2S&MPT-2 (Worcestershire, UK) at room temperature. X-ray photoelectron spectroscopy (XPS) was carried out on a K-Alpha 1063 electron spectrometer (Al Kα), and the resulting data was calibrated by the C 1s peak band of polluted carbon at 284.6 eV. The content of −SH was measured by Ellman test with a spectrophotometer (JH721, China). The magnetic properties of the samples were investigated at 300 K using a vibrating sample magnetometer (VSM).

MTT assay was used to evaluate cell toxicity of Fe_3O_4 nanoparticles before and after functionalization. The MNPs (Fe_3O_4, Fe_3O_4@DMSA, Fe_3O_4@SiO_2, and Fe_3O_4@SiO_2@DMSA) at varying concentrations (15.6, 62.5, 250.0, and 1000.0 mg/L) were prepared in PBS. L929 fibroblast cells were seeded in 96-well plates (5000 cells per well) in DMEM medium (100 μL per well) for 24 h. Then, 50 μL of DMEM medium of each well was displaced with 50 μL of nanoparticle solution (experimental groups), PBS (negative control), or DMSO (positive control). After incubation for 24, 36, 48, 60, and 72 h, 20 μL of MTT was added to each well and incubated for another 4 h. Culture media was replaced by DMSO (150 μL). All incubations were carried out at 37 °C and 5% CO_2. The images of cell lines were acquired at 400× magnification by an Olympus IX71 microscope. The MTT assay was performed, and the optical density (OD) values were measured at 490 nm. The cell relative growth rate (RGR) was calculated as follows:[26]

$$\mathrm{RGR}\ (\%) = \frac{(\mathrm{OD\ of\ experimental\ group})}{(\mathrm{OD\ of\ negative\ control\ group})} \times 100\%$$

Fresh human blood was provided by Haikou People's Hospital (Hainan, China). Then, EDTA anticoagulated blood was diluted at a dilution ratio of 8 mL of blood to 10 mL of normal saline. The MNPs (Fe_3O_4, Fe_3O_4@DMSA, Fe_3O_4@SiO_2, and Fe_3O_4@SiO_2@DMSA) were lixiviated with 0.9% saline, with a range of concentrations corresponding to 62.5, 250.0, 1000.0, 3000.0, 5000.0, and 7000.0 mg/L. Then, 25 μL of diluted blood was added to each tube containing 1 mL of materials solution (experimental groups), 0.9% saline (negative control), and distilled water (positive control). After incubation for 150 min at 37 °C, the tubes were centrifuged at 10 g/min for 5 min. Then, 200 μL of supernatant of each tube was added to 96-well plates, and OD values were measured at 540 nm. The hemolysis rate (HR) was calculated using the mean OD value for each group as follows:[27]

$$\mathrm{HR}(\%) = \frac{(\mathrm{OD\ of\ experimental\ group} - \mathrm{OD\ of\ negative\ group})}{(\mathrm{OD\ of\ positive\ group} - \mathrm{OD\ of\ negative\ group})} \times 100\%$$

All experiments were performed at least five times, and the data was averaged and expressed as mean ± standard deviation (SD).

RESULTS AND DISCUSSION

Characterization of Sulfhydryl-Modified Fe_3O_4@SiO_2 MNPs. TEM was used to observe the structure of Fe_3O_4,

DOI: 10.1021/acsami.5b03873
ACS Appl. Mater. Interfaces 2015, 7, 14983−14991

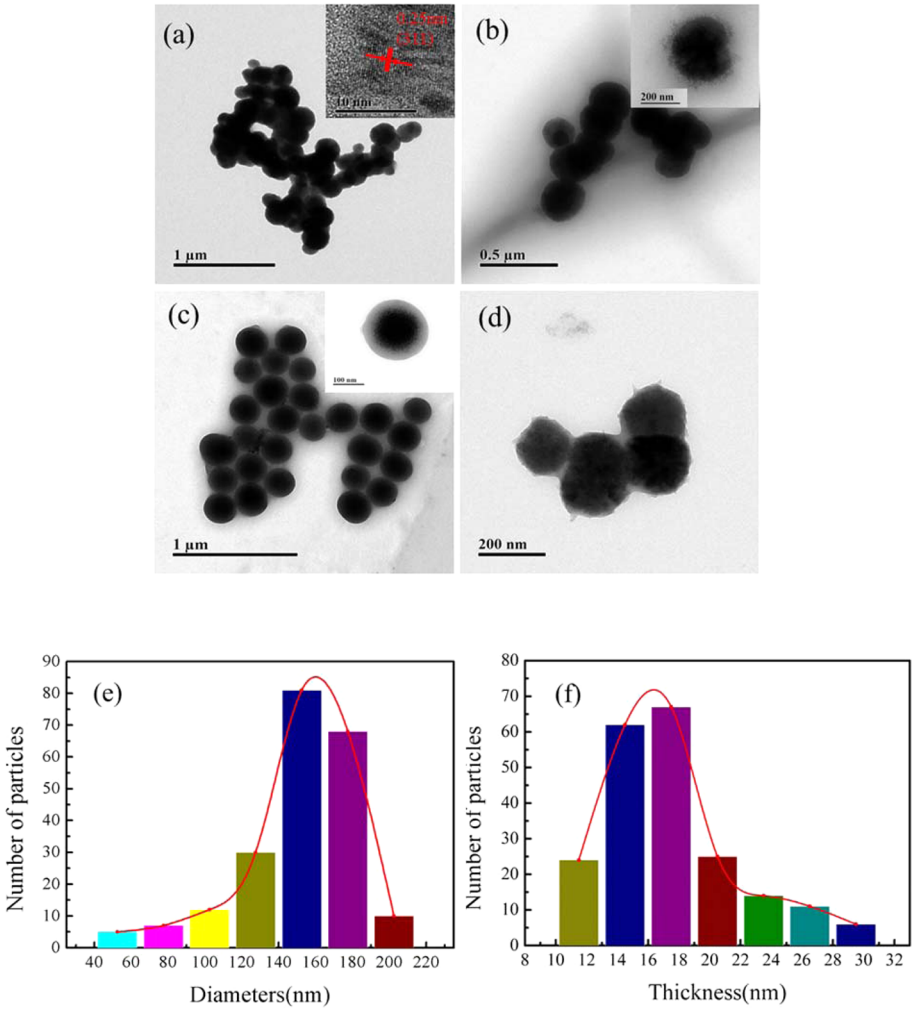

Figure 1. TEM images of (a) Fe_3O_4, (b) Fe_3O_4@DMSA, (c) Fe_3O_4@SiO_2, and (d) Fe_3O_4@SiO_2@DMSA nanoparticles. (e) Size distributions of Fe_3O_4 core. (f) Thickness distributions of SiO_2 shell.

Fe_3O_4@DMSA, Fe_3O_4@SiO_2, and Fe_3O_4@SiO_2@DMSA MNPs; the results are shown in Figure 1. The TEM image shows that the Fe_3O_4 particles have a mean diameter about 150−200 nm (Figure 1a,e). In addition, the high-resolution TEM (HRTEM) image shows clear 2D lattice fringes of the magnetite material. The interplanar spacing is about 0.251 nm, which corresponds well to the (311) lattice plane of the inverse spinel structure of Fe_3O_4 (Figure 1a, inset). After the coating process, the presence of silica layers of around 15−19 nm can be easily seen at the periphery of MNPs (Figure 1c,f). This core−shell feature elucidates that the Fe_3O_4 nanoparticles are well-embedded inside rather than impling that they are adhering physically or blending into the silica. After DMSA modification, a thin and furry layer of DMSA is formed on the surface of the Fe_3O_4 and Fe_3O_4@SiO_2 nanoparticles. The diameters of Fe_3O_4 and Fe_3O_4@SiO_2 nanoparticles are changed, but the aggregation between the particles is improved (Figure 1b,d).

Figure 2 shows the XRD patterns of Fe_3O_4, Fe_3O_4@DMSA, Fe_3O_4@SiO_2, and Fe_3O_4@SiO_2@DMSA MNPs. It is seen that all the samples exhibit identical cubic inverse spinel structures,[28] indicating that the modification does not induce any obvious change of the crystal structure of the magnetic nanoparticles primarily.

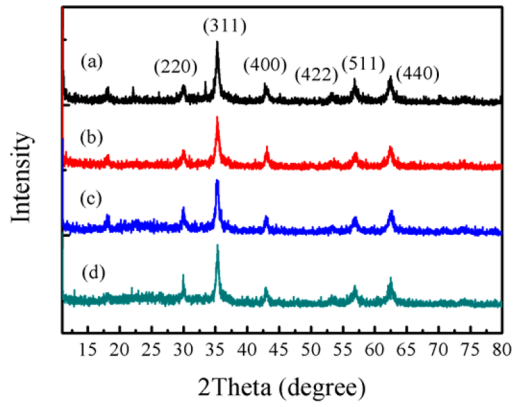

Figure 2. XRD patterns of (a) Fe_3O_4, (b) Fe_3O_4@DMSA, (c) Fe_3O_4@SiO_2, and (d) Fe_3O_4@SiO_2@DMSA MNPs.

Figure 3 shows the FTIR spectrum of four kinds of nanoparticles (Fe_3O_4, Fe_3O_4@DMSA, Fe_3O_4@SiO_2, and Fe_3O_4@SiO_2@DMSA) and DMSA. In the Fe_3O_4 curve, the peak around 588 cm^{-1} is assigned to the typical Fe−O vibration of the Fe_3O_4 MNPs, and the peaks at 1625 and 3415 cm^{-1} are related to the −OH bending vibration and stretching vibration of water molecules and −OH groups on the particle surface (Figure 3b).[29−31] The pronounced changes upon addition of

DOI: 10.1021/acsami.5b03873
ACS Appl. Mater. Interfaces 2015, 7, 14983−14991

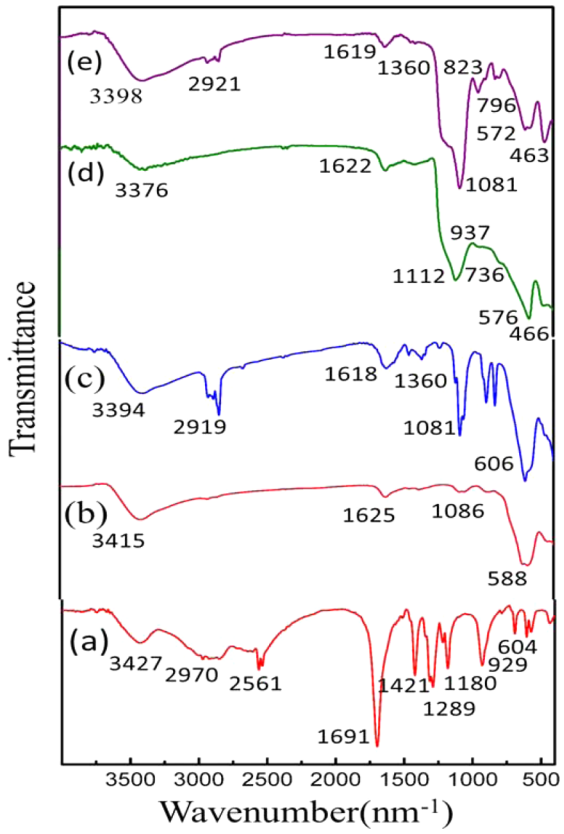

Figure 3. FT-IR spectra of (a) DMSA, (b) Fe_3O_4, (c) Fe_3O_4@DMSA, (d) Fe_3O_4@SiO_2, and (e) Fe_3O_4@SiO_2@DMSA MNPs.

the silica shell can be identified by the appearance of O−Si−O bending mode as well as Si−O−Si symmetric, Si−O symmetric, and Si−O−Si asymmetric stretching modes observed at 466, 786, 937, and 1112 cm^{-1}, respectively (Figure 3d).[29−31] In the Fe_3O_4@DMSA and Fe_3O_4@SiO_2@DMSA curves (Figure 3c,e), the peaks at 1619 and 1360 cm^{-1} are attributed to the asymmetric and symmetric stretching mode of $-COO^-$ groups, whereas the peaks at 1691 and 1421 cm^{-1} in the DMSA curve are related to −COOH groups (Figure 3a), which suggests that DMSA molecules are bound to the particle surface via $-COO^-$ groups.[32−34] Because most of thiol groups have been oxidized into disulfide groups, the peaks of thiol and disulfide groups are not found in the curves shown in Figure 3c,e.[24,32,33]

Figure 4 gives the broad- and narrow-scan XPS spectra of DMSA functionalized Fe_3O_4@SiO_2 nanocomposites. The peaks at 103.08 and 533.08 eV are assigned to Si 2p and O 1s, respectively. There are no peaks at 711.02 and 724.04 eV that are the characteristic doublets of Fe $2p_{3/2}$ and Fe $2p_{1/2}$ of iron oxide in the curve, which is referenced to reported values of Fe_3O_4 in the literature.[30] This indicates that the SiO_2 coating layer is deposited on the Fe_3O_4 surface, forming an integral core/shell structure. The changes upon DMSA modification can be identified by the appearance of the peaks at 154.08 and 285.08 eV, which are considered to be S 2p and C 1s according to ref 35.

From the C 1s spectra of the Fe_3O_4@SiO_2@DMSA magnetic particles (Figure 4b), it is seen that the sample exhibits peaks at 284.83 and 289.90 eV assigned to −C−O and −C═O of C4, respectively. In addition, the peak at 286.60 eV assigned to the C atoms of C−H and SiO_2 mixture can also be identified for the sample.[35] In the O 1s spectra (Figure 4c), the peak at ∼532.60 eV is assigned to O of SiO_2, and the peaks at 530.40 and 534.00 eV are supposed to originate from the oxygen

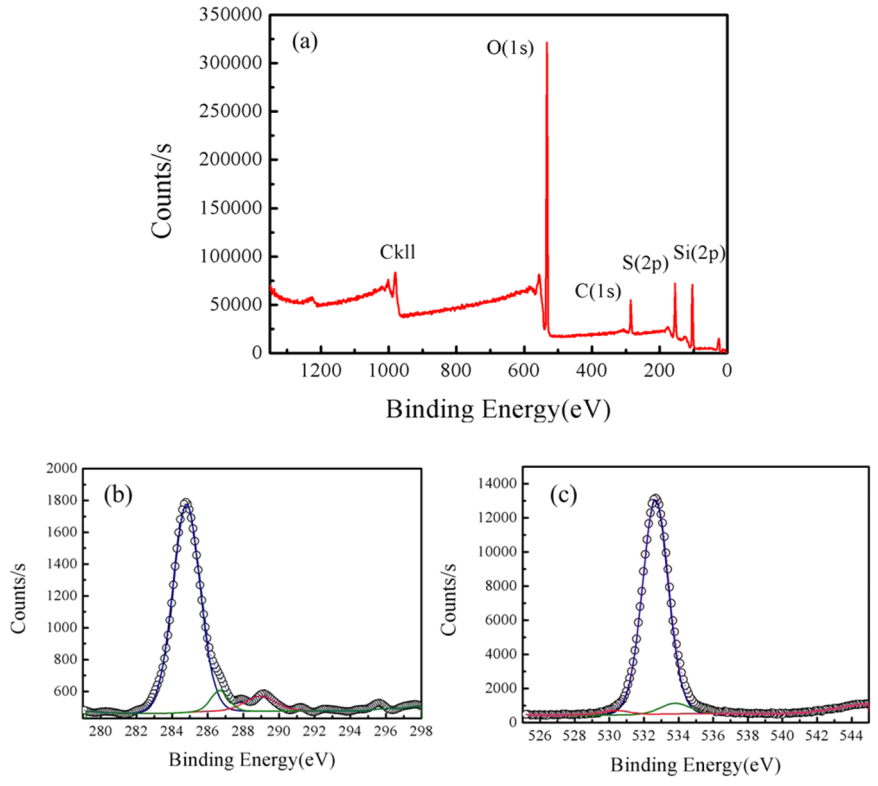

Figure 4. XPS (a) broad-scan spectra, (b) narrow scan for C 1s, and (c) narrow scan for O 1s of Fe_3O_4@SiO_2@DMSA MNPs.

DOI: 10.1021/acsami.5b03873
ACS Appl. Mater. Interfaces 2015, 7, 14983−14991

atoms in −COOR.[35] It is obvious that the particle surface contains O and C, proving the surface modification of DMSA.

Figure 5 shows the standard curve obtained for the quantification of sulfhydryl groups according to the method

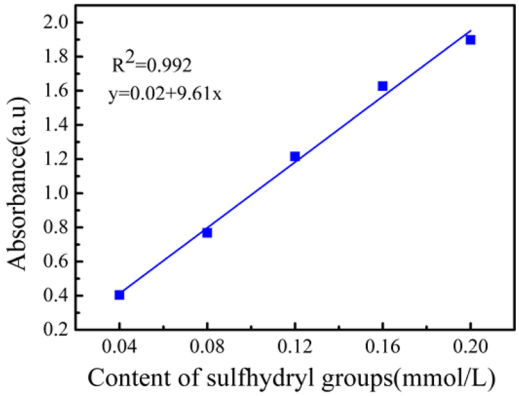

Figure 5. Standard curve obtained for the quantification of sulfhydryl groups.

of Ellman's test using the spectrophotometer.[36] The content of sulfhydryl on the surface of Fe_3O_4@DMSA and Fe_3O_4@SiO_2@DMSA nanoparticles are calculated to be 0.079 and 0.089 mmol/g, respectively (Table 1), which is more than the value

Table 1. Content of Sulfhydryl Groups on the Surface of DMSA-Modified MNPs

MNPs	absorbance (a.u.)	content of −SH groups (mmol/g)
Fe_3O_4@DMSA	0.326	0.079
Fe_3O_4@SiO_2@DMSA	0.361	0.089

of 0.048 mmol/g for MNPs synthesized by other researchers.[37] The results also show that the content of sulfhydryl of Fe_3O_4@SiO_2@DMSA is higher than that of Fe_3O_4@DMSA, indicating a larger number of binding sites on the SiO_2 shell than that of naked Fe_3O_4.

Zeta potential measurements as a function of pH for the Fe_3O_4, Fe_3O_4@DMSA, Fe_3O_4@SiO_2, and Fe_3O_4@SiO_2@DMSA nanoparticles are shown in Figure 6. Curves show that the surface potential of all nanoparticles decreases to 0 mV under pH 3.6 as pH decreases from 11.0, indicating its excellent dispersibility and stability. This is because the reduction in zeta

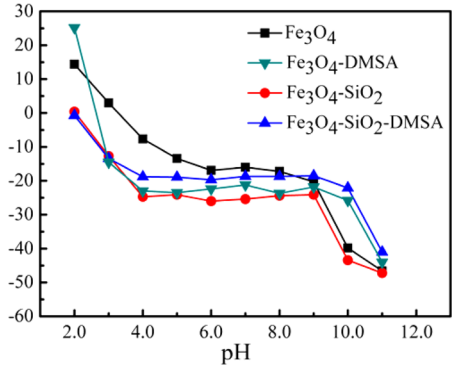

Figure 6. Dependence of zeta spectra of Fe_3O_4, Fe_3O_4@DMSA, Fe_3O_4@SiO_2, and Fe_3O_4@SiO_2@DMSA MNPs on the change of pH.

potential is in good agreement with the reduction in physical stability.[38] In addition, the colloidal system is not stable at the isoelectric point (IEP) because there are no interparticle repulsive forces, which is due to the absence of particle surface charges.[39] In the case of the SiO_2-coated nanoparticles, it is noted that the particles are negatively charged at acidic pH with a surface potential greater than −25 mV at pH <4.0, and its IEP is low to pH 2.0. This confirms the presence of silica on the particle surface and thus enhanced stability. Although the zeta potential of −SH-modified Fe_3O_4@SiO_2 nanoparticles decreases compared to that of the unmodified particles, this is possible because some Si−OH groups have been replaced by sulfhydryl groups. The zeta potential of both DMSA-modified particles (Fe_3O_4@DMSA and Fe_3O_4@SiO_2@DMSA) are lower than that of the unmodified ones at pH >9.0, indicating that the stability of nanoparticles cannot be improved by DMSA modification under highly alkaline conditions.

The correlation of zeta potential to pH is important to know so that one can predict how the varying pH inside the human body will affect the surface charge of the nanoparticles and because it affects protein adsorption onto nanoparticles. Previous studies indicate that nanoparticles with positive zeta potential displayed good protein adsorption, whereas the negatively charged samples did not significantly adsorb protein.[39]

Dynamic light scattering (DLS) measurements (Figure 7) of the dispersed Fe_3O_4 nanoparticles show that before surface modification (Figure 7a) the Fe_3O_4 and Fe_3O_4@SiO_2 nanoparticles in PBS have an average hydrodynamic diameter of 783 and 613 nm rather than arranged 200 nm described in TEM results that is due to the aggregation taking place when the particles are transferred to PBS.[40] After DMSA modification, the hydrodynamic diameters of Fe_3O_4 and Fe_3O_4@SiO_2 nanoparticles decrease to 420 and 451 nm, indicating that the improvement of particle aggregation is a result of the increased hydrophility.[40]

Nanoparticle physicochemical properties in a physiological medium can vary because of protein adsorption to the nanoparticle surface; this forms the so-called protein corona, which can influence nanoparticle stability, uptake, and toxicity.[41,42] We analyzed MNP hydrodynamic size in complete culture medium (Figure 7b) and size variations two times in the first and third days (Figure 7c). Note that the hydrodynamic size in culture medium shows results similar to those in PBS. MNP incubation in medium leads to an increase in hydrodynamic size; this effect is probably due to the adsorption of a large amount of protein.[41]

Preserving the magnetic property is an important parameter for surface engineering of magnetic nanoparticles. The magnetization curves of the nanoparticles are shown in Figure 8. The value of saturation magnetization of Fe_3O_4 was calculated to be 66.15 emu/g; the level of saturation magnetization of SiO_2-coated Fe_3O_4 MNPs was reduced to 42.95 emu/g (Fe_3O_4@SiO_2) and 39.81 emu/g (Fe_3O_4@SiO_2@DMSA) because of the silica coating. The modification of DMSA did not cause a significant decrease of the nanoparticle magnetization saturation.

Hemolysis Assay. Hemocompatibility is of great importance for the biomaterials required to contact blood. In this study, hemolysis studies performed on the particles demonstrate that coating the particles with a SiO_2 layer can reduce the occurrence of red blood cell (RBC) lysis compared to the effect of uncoated particles. In addition, the DMSA modification

DOI: 10.1021/acsami.5b03873
ACS Appl. Mater. Interfaces 2015, 7, 14983−14991

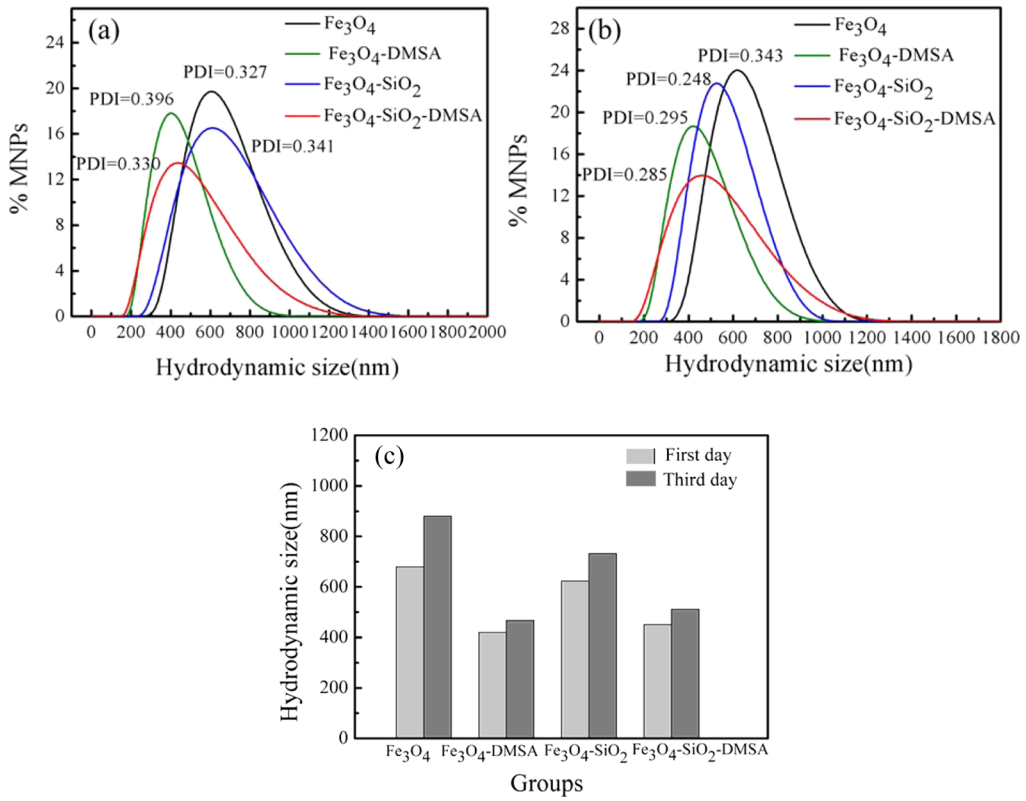

Figure 7. Hydrodynamic diameter of (a) nanoparticles in PBS, (b) nanoparticles in complete culture medium, and (c) nanoparticles in complete culture medium at two incubation times, determined by DLS. Data are represented as mean hydrodynamic size. PDI, polydispersity index.

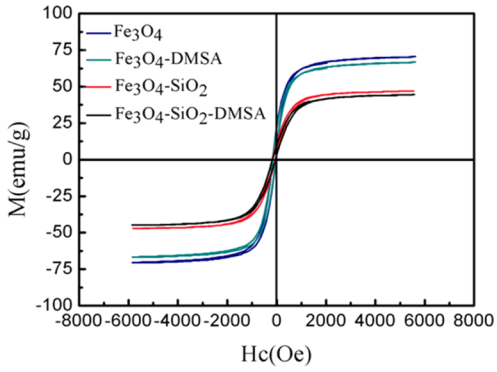

Figure 8. Field-dependent magnetization measurement of Fe_3O_4, Fe_3O_4@DMSA, Fe_3O_4@SiO_2, and Fe_3O_4@SiO_2@DMSA.

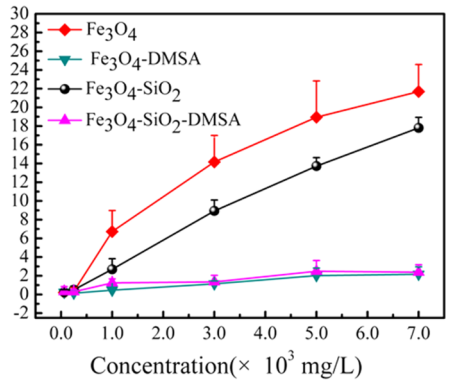

Figure 9. Results of hemolytic test of nanoparticles at different concentrations.

process can further decrease hemolysis (Figure 9). The hemolysis rates of Fe_3O_4 were more than 5.00% at a low particle concentration of 1000.0 mg/L. The hemolysis rates of naked Fe_3O_4 and Fe_3O_4@SiO_2 particles are up to 21.69 and 17.81%, respectively, at a particle concentration of 7000.0 mg/L. However, it is apparent that even at a particle concentration of 7000.0 mg/L the hemolysis rates of Fe_3O_4@DMSA and Fe_3O_4@SiO_2@DMSA particles are less than 5.00% at 2.15 and 2.37%, respectively, indicating that DMSA-modified Fe_3O_4 and Fe_3O_4@SiO_2 magnetic particles do not cause significant hemolysis and have good hemocompatibility, which may enable them to be used for various biomedical applications.

Cytotoxicity Test. The cytotoxicity of magnetic nanoparticles were investigated with low particle doses or short incubation times by many studies and showed little reduction in cell viability. Here, we use different concentrations and different incubation times. L929 fibroblast cell viability decreases with the increase of time and concentration (Figure 10). When the particle concentration was increased up to 1000.0 mg/L, cell viability decreased to less than 75% after 72 h of incubation. The study demonstrates that the DMSA-modified particles can improve cytotoxicity compared to Fe_3O_4 and Fe_3O_4@SiO_2 magnetic particles. In addition, the cell viability decreases when magnetic particles are modified with the SiO_2 coating layer. The DMSA-modified Fe_3O_4@SiO_2 magnetic particles show slightly significant effect on cell viability even at extremely high concentration and long incubation time.

Because of the large surface-area-to-volume ratio, the magnetic nanoparticles tend to agglomerate and adsorb proteins.[43] The dark-brown color in the cell image (Figure 11) appears on the surface of cells owing to the agglomeration of magnetic nanoparticles, which corresponds to the TEM and

DOI: 10.1021/acsami.5b03873
ACS Appl. Mater. Interfaces 2015, 7, 14983−14991

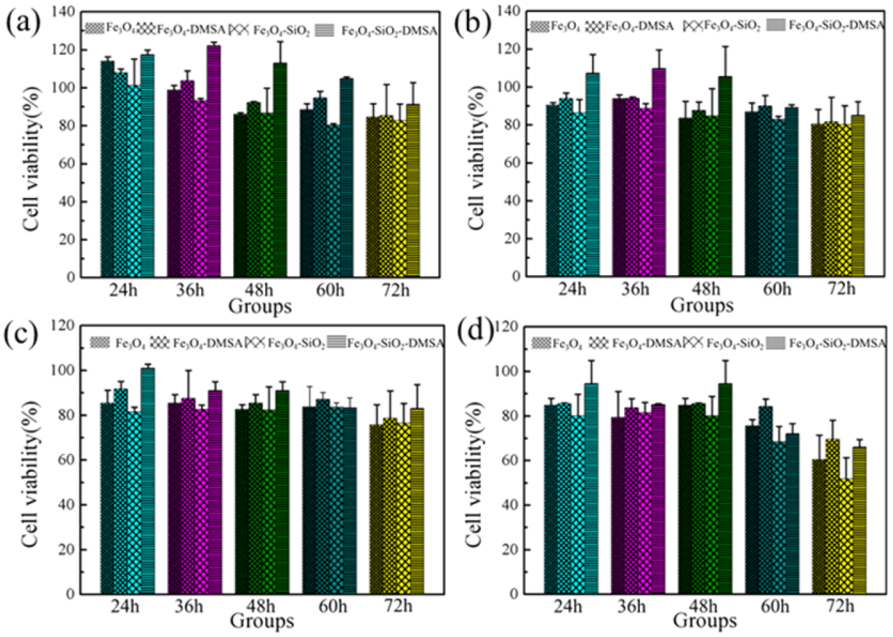

Figure 10. MTT assay of L929 fibroblast cell viability after treatment with the nanoparticles at concentrations of (a–d) 16.5, 62.5, 250.0, and 1000.0 mg/L, respectively, for 24, 36, 48, 60, and 72 h.

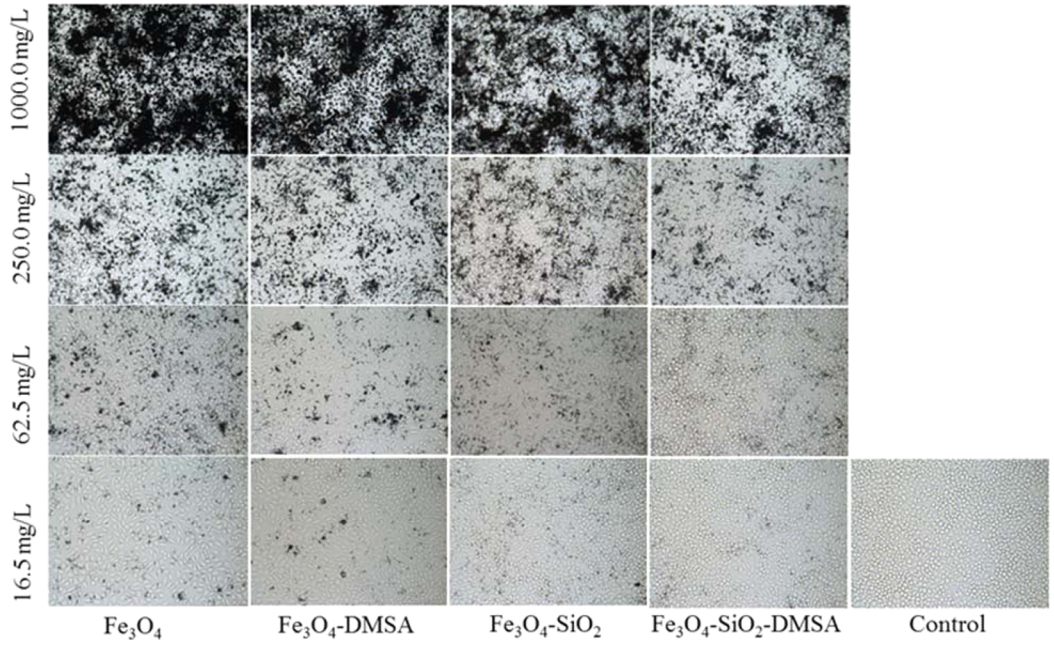

Figure 11. Bright-field microscopy of L929 fibroblast cell images with 400× magnification after incubating with nanoparticles at concentrations of 16.5, 62.5, 250.0, and 1000.0 mg/L for 72 h.

DLS results. The following plausible explanations can support our observations of cytotoxicity effects as reported earlier by Pisanic et al.:[44] The presence of magnetic nanoparticles in or on the cells may obstruct transcriptional regulation and protein synthesis, resulting in cell death. In addition, nanoparticle stability, uptake, and toxicity can be dramatically influenced by protein adsorption to the nanoparticle surface, which forms the so-called protein corona.[41,45] After functionalization with negatively charged groups (carboxylate, sulfate, phosphate, etc.), the magnetic particles are immediately covered by different proteins according to their different protein affinity when in contact with biological fluids.[46]Thus, according to the zeta potential measurements and DLS measurements, the sulfhydryl-modified magnetic particles dramatically reduce the interaction among surfactant, the nanostructures, and the cellular components because of their different surface charge and protein affinity compared with Fe_3O_4 and Fe_3O_4@SiO_2 magnetic particles.

CONCLUSIONS

A simple facile approach for the preparation of DMSA-modified Fe_3O_4@SiO_2 core/shell structure magnetic particles by a soft chemical approach was investigated in this study. The detailed structural analyses by TEM, XRD, FTIR, XPS, zeta potential

DOI: 10.1021/acsami.5b03873
ACS Appl. Mater. Interfaces 2015, 7, 14983–14991

measurements, DLS, and VSM confirm the successful functionalization of Fe_3O_4@SiO_2 nanoparticles with sulfhydryl. The size of the sulfhydryl-modified Fe_3O_4@SiO_2 magnetic particles could be tuned with core diameter of 150−200 nm and layer thickness of 15−19 nm. FTIR and XPS results show that DMSA molecules were bound to the particle surface via COO^- groups. These nanoparticles exhibit fine colloidal stability, enhanced dispersibility, and optimal magnetization by zeta potential measurements, DLS, and VSM measurements. In addition, the cytocompatibility and hemocompatibility of sulfhydryl-modified Fe_3O_4@SiO_2 magnetic particles are significantly improved after surface modification with sulfhydryl groups. Hemolysis rates of Fe_3O_4@SiO_2@DMSA particles are 2.37% at a particle concentration of 7000.0 mg/mL, indicating that DMSA-modified Fe_3O_4@SiO_2 magnetic particles do not cause significant hemolysis and have good hemocompatibility. The cytotoxicity test demonstrates that the DMSA-modified Fe_3O_4@SiO_2 magnetic particles show a slightly significant effect to cell viability even at extremely high concentration and long incubation time. The above features are highly conducive for application of these magnetic nanoparticles to biomedical fields.

AUTHOR INFORMATION

Corresponding Author

*Metallurgical Building 226, Central South University, Lushan South Road, Yuelu District, Changsha, Hunan, China. Tel.: +86 731 88877863. Fax: +86 731 88836207. E-mail: xyguo@csu.edu.cn.

Funding

International S&T Cooperation Program of China, 2013DFA51290

Notes

The authors declare no competing financial interest.

ABBREVIATIONS

DMSA, the meso-2, 3-dimercaptosuccinic acid; MNPs, magnetic nanoparticles; MTT, 3-(4, 5-dimethylthiazol-2-yl)-2, 5-diphenyltetrazolium bromide

REFERENCES

(1) Kim, M. I.; Shim, J.; Li, T.; Lee, J.; Park, H. G. Fabrication of Nonporous Nanocomposites Entrapping Fe_3O_4 Magnetic Nanoparticles and Oxidases for Colorimetric Biosensing. *Chem.-Eur. J.* **2011**, *17*, 10700−10707.

(2) Ding, J.; Zhao, J.; Cheng, K.; Cheng, K.; Liu, G.; Xiu, D. In Vivo Photodynamic Therapy and Magnetic Resonance Imaging of Cancer by TSPP-Coated Fe_3O_4 Nanoconjugates. *J. Biomed Nanotechnol.* **2010**, *6*, 683−686.

(3) Charan, S.; Kuo, C. W.; Kuo, Y. W.; Singh, N.; Drake, P.; Lin, Y. J.; Chen, P. Synthesis of Surface Enhanced Raman Scattering Active Magnetic Nanoparticles for Cell Labeling and Sorting. *J. Appl. Phys.* **2009**, *105*, 07−10.

(4) Veiseh, O.; Gunn, J. W.; Zhang, M. Design and Fabrication of Magnetic Nanoparticles for Targeted Drug Delivery and Imaging. *Adv. Drug Delivery Rev.* **2010**, *62*, 284−304.

(5) Bao, J.; Chen, W.; Liu, T.; Zhu, Y.; Jin, P.; Wang, L.; Li, Y.; Wei, Y.; Li, Y. Bifunctional Au-Fe_3O_4 Nanoparticles for Protein Separation. *ACS Nano* **2007**, *1*, 293−298.

(6) Singh, N.; Jenkins, G. J. S.; Asadi, R.; Doak, S. H. Potential Toxicity of Superparamagnetic Iron Oxide Nanoparticles (SPION). *Nano Rev.* **2010**, 1.

(7) Soenen, S. J. H.; Himmelreich, U.; Nuytten, N.; De Cuyper, M. Cytotoxic Effects of Iron Oxide Nanoparticles and Implications for Safety in Cell Labelling. *Biomaterials* **2011**, *32*, 195−205.

(8) Arora, S.; Rajwade, J. M.; Paknikar, K. M. Nanotoxicology and in Vitro Studies: The Need of the Hour. *Toxicol. Appl. Pharmacol.* **2012**, *258*, 151−165.

(9) Love, S. A.; Maurer-Jones, M. A.; Thompson, J. W.; Lin, Y. S.; Haynes, C. L. Assessing Nanoparticle Toxicity. *Ann. Rev. Anal. Chem.* **2012**, *5*, 181−205.

(10) An, Q.; Yu, M.; Zhang, Y.; Ma, W.; Guo, J.; Wang, C. Fe_3O_4@Carbon Microsphere Supported Ag-Au Bimetallic Nanocrystals with the Enhanced Catalytic Activity and Selectivity for the Reduction of Nitroaromatic Compounds. *J. Phys. Chem. C* **2011**, *116*, 22432−22440.

(11) Chen, Y. J.; Xiao, G.; Wang, T. S.; Ouyang, Q. Y.; Qi, L. H.; Ma, Y.; Gao, P.; Zhu, C. L.; Cao, M. S.; Jin, H. B. Porous Fe_3O_4/Carbon Core/Shell Nanorods: Synthesis and Electromagnetic Properties. *J. Phys. Chem. C* **2011**, *115*, 13603−13608.

(12) Wang, C.; Daimon, H.; Sun, S. Dumbbell-Like Pt-Fe_3O_4 Nanoparticles and Their Enhanced Catalysis for Oxygen Reduction Reaction. *Nano Lett.* **2009**, *9*, 1493−1496.

(13) Zhu, C. L.; Zhang, M. L.; Qiao, Y. J.; Xiao, G.; Zhang, F.; Chen, Y. J. Fe_3O_4/TiO_2 Core/Shell Nanotubes: Synthesis and Magnetic and Electromagnetic Wave Absorption Characteristics. *J. Phys. Chem. C* **2010**, *114*, 16229−16235.

(14) Qu, J.; Liu, G.; Wang, Y.; Hong, R. Preparation of Fe_3O_4-Chitosan Nanoparticles Used for Hyperthermia. *Adv. Powder Technol.* **2010**, *21*, 461−467.

(15) Morel, A. L.; Nikitenko, S. I.; Gionnet, K.; Wattiaux, A.; Lai-Kee-Him, J.; Labrugere, C.; Chevalier, B.; Deleris, G.; Petibois, C.; Brisson, A.; Simonoff, M. Sonochemical Approach to the Synthesis of Fe_3O_4@SiO_2 Core-Shell Nanoparticles with Tunable Properties. *ACS Nano* **2008**, *2*, 847−856.

(16) Wang, J.; Zheng, S.; Shao, Y.; Liu, J.; Xu, Z.; Zhu, D. Amino-Functionalized Fe_3O_4@SiO_2 Core-Shell Magnetic Nanomaterial as a Novel Adsorbent for Aqueous Heavy Metals Removal. *J. Colloid Interface Sci.* **2010**, *349*, 293.

(17) Zhou, L.; Gao, C.; Xu, W. Robust Fe_3O_4/SiO_2-Pt/Au/Pd Magnetic Nanocatalysts with Multifunctional Hyperbranched Polyglycerol Amplifiers. *Langmuir* **2010**, *26*, 11217−11225.

(18) Lei, Z.; Ren, N.; Li, Y.; Li, N.; Mu, B. Fe_3O_4/SiO_2-g-PSStNa Polymer Nanocomposite Microspheres (PNCMs) from a Surface-Initiated Atom Transfer Radical Polymerization (SI-ATRP) Approach for Pectinase Immobilization. *J. Agric. Food Chem.* **2009**, *57*, 1544−1549.

(19) Zhu, Y.; Fang, Y.; Kaskel, S. Folate-Conjugated Fe_3O_4@SiO_2 Hollow Mesoporous Spheres for Targeted Anticancer Drug Delivery. *J. Phys. Chem. C* **2010**, *114*, 16382−16388.

(20) Shin, S.; Jang, J. Thiol Containing Polymer Encapsulated Magnetic Nanoparticles as Reusable and Efficiently Separable Adsorbent for Heavy Metal Ions. *Chem. Commun.* **2007**, 4230−4232.

(21) Du, J.; Jing, C. Preparation of Thiol Modified Fe_3O_4@Ag Magnetic SERS Probe for PAHs Detection and Identification. *J. Phys. Chem. C* **2011**, *115*, 17829−17835.

(22) Zhao, X.; Cai, Y.; Wang, T.; Shi, Y.; Jiang, G. Preparation of Alkanethiolate-Functionalized Core/Shell Fe_3O_4@Au Nanoparticles and Its Interaction with Several Typical Target Molecules. *Anal. Chem.* **2008**, *80*, 9091−9096.

(23) Mejías, R.; Gutiérrez, L.; Salas, G.; Pérez, Y. S.; Zotes, T. M.; Lázaro, F. J.; María, P. M.; Barber, D. F. Long Term Biotransformation and Toxicity of Dimercaptosuccinic Acid-Coated Magnetic Nanoparticles Support Their Use in Biomedical Applications. *J. Controlled Release* **2013**, *171*, 225−233.

(24) Jaiswal, M. K.; Mehta, S.; Banerjee, R.; Bahadur, D. A. Comparative Study on Thermoresponsive Magnetic Nanohydrogels: Role of Surface-Engineered Magnetic Nanoparticles. *Colloid Polym. Sci.* **2012**, *290*, 607−617.

(25) Liu, Y.; Wang, J. Comparative and Quantitative Investigation of Cell Labeling of a 12-nm DMSA-Coated Fe_3O_4 Magnetic Nanoparticle with Multiple Mammalian Cell Lines. *J. Mater. Res.* **2011**, *26*, 822−831.

(26) Pieters, R.; Loonen, A. H.; Huismans, D. R.; Broekema, G. J.; Dirven, M. W.; Heyenbrok, M. W.; Hahlen, K.; Veerman, A. J. In Vitro Drug Sensitivity of Cells from Children with Leukemia Using the

DOI: 10.1021/acsami.5b03873
ACS Appl. Mater. Interfaces 2015, 7, 14983−14991

MTT Assay with Improved Culture Conditions. *Blood* **1990**, *76*, 2327−2336.
(27) Wu, W.; Chen, B.; Cheng, J.; Wang, J.; Xu, W.; Liu, L.; Xia, G.; Wei, H.; Wang, X.; Yang, M.; Yang, L.; Zhang, Y.; Xu, C.; Li, J. Biocompatibility of Fe_3O_4/DNR Magnetic Nanoparticles in the Treatment of Hematologic Malignancies. *Int. J. Nanomed.* **2010**, *5*, 1079.
(28) Yang, C.; Wang, G.; Lu, Z.; Sun, J.; Zhuang, J.; Yang, W. Effect of Ultrasonic Treatment on Dispersibility of Fe_3O_4 Nanoparticles and Synthesis of Multi-Core Fe_3O_4/SiO_2 Core/Shell Nanoparticles. *J. Mater. Chem.* **2005**, *15*, 4252−4257.
(29) Sharma, R. K.; Puri, A.; Monga, Y.; Adholeya, A. Acetoacetanilide-Functionalized Fe_3O_4 Nanoparticles for Selective and Cyclic Removal of Pb^{2+} Ions from Different Charged Wastewaters. *J. Mater. Chem. A* **2014**, *2*, 12888−12898.
(30) Du, G. H.; Liu, Z. L.; Xia, X.; Chu, Q.; Zhang, S. M. Characterization and Application of Fe_3O_4/SiO_2 Nanocomposites. *J. Sol-Gel Sci. Technol.* **2006**, *39*, 285−291.
(31) Zhao, L.; Liu, H.; Wang, F.; Zeng, L. Design of Yolk-Shell Fe_3O_4@PMAA Composite Microspheres for Adsorption of Metal Ions and pH-Controlled Drug Delivery. *J. Mater. Chem. A* **2014**, *2*, 7065−7074.
(32) Fatahian, S.; Shahbazi-Gahrouei, D.; Pouladian, M.; Yousefi, M. H.; Amiri, G. R.; Noori, A. Biodistribution and Toxicity Assessment of Radiolabeled and DMSA Coated Ferrite Nanoparticles in Mice. *J. Radioanal. Nucl. Chem.* **2012**, *293*, 915−921.
(33) Kim, M.; Lim, B.; Jeong, Y.; Cho, Y. W.; Choa, Y. Surface Modification of Magnetite Nanoparticles for Immobilization with lysozyme. *J. Ceram. Process. Res.* **2007**, *8*, 293.
(34) Chen, W.; Yi, P.; Zhang, Y.; Zhang, L.; Deng, Z.; Zhang, Z. Composites of Amino Dextran-Coated Fe_3O_4 Nanoparticles and Graphene Oxide for Cellular Magnetic Resonance Imaging. *ACS Appl. Mater. Interfaces* **2011**, *3*, 4085−4091.
(35) Chastain, J.; King, R. C. *Handbook of X-ray Photoelectron Spectroscopy: A Reference Book of Standard Spectra for Identification and Interpretation of XPS Data*; Perkin-Elmer, Eden Prairie, MN, 1992; p 261.
(36) Bulaj, G.; Kortemme, T.; Goldenberg, D. P. Ionization-Reactivity Relationships for Cysteine Thiols in Polypeptides. *Biochemistry* **1998**, *37*, 8965−8972.
(37) Dong, W.; Li, Y.; Niu, D.; Ma, Z.; Gu, J.; Chen, Y.; Zhao, W. Facile Synthesis of Monodisperse Superparamagnetic Fe_3O_4 Core@Hybrid@Au Shell Nanocomposite for Bimodal Imaging and Photothermal Therapy. *Adv. Mater.* **2011**, *23*, 5392−5397.
(38) Freitas, C.; Müller, R. H. Effect of Light and Temperature on Zeta Potential and Physical Stability in Solid Lipid Nanoparticle (SLN) Dispersions. *Int. J. Pharm.* **1998**, *168*, 221−229.
(39) Patil, S.; Sandberg, A.; Heckert, E.; Self, W.; Seal, S. Protein Adsorption and Cellular Uptake of Cerium Oxide Nanoparticles as a Function of Zeta Potential. *Biomaterials* **2007**, *28*, 4600−4607.
(40) Xie, J.; Xu, C.; Xu, Z.; Hou, Y.; Young, K. L.; Wang, S. X.; Pourmand, N.; Sun, S. Linking Hydrophilic Macromolecules to Monodisperse Magnetite (Fe_3O_4) Nanoparticles via Trichloros-Triazine. *Chem. Mater.* **2006**, *18*, 5401−5403.
(41) Mahmoudi, M.; Lynch, I.; Ejtehadi, M. R.; Monopoli, M. P.; Bombelli, F. B.; Laurent, S. Protein-Nanoparticle Interactions: Opportunities and Challenges. *Chem. Rev.* **2011**, *111*, 5610−5637.
(42) Jedlovszky-Hajdú, A.; Bombelli, F. B.; Monopoli, M. P.; Tombácz, E.; Dawson, K. A. Surface Coatings Shape the Protein Corona of SPIONs with Relevance to Their Application in Vivo. *Langmuir* **2012**, *28*, 14983−14991.
(43) Gupta, A. K.; Wells, S. Surface-Modified Superparamagnetic Nanoparticles for Drug Delivery: Preparation, Characterization, and Cytotoxicity Studies. *IEEE Trans. NanoBioscience* **2004**, *3*, 66−73.
(44) Ankamwar, B.; Lai, T. C.; Huang, J. H.; Liu, R. S.; Hsiao, M.; Chen, C. H.; Hwu, Y. K. Biocompatibility of Fe_3O_4 Nanoparticles Evaluated by in Vitro Cytotoxicity Assays Using Normal, Glia and Breast Cancer Cells. *Nanotechnology* **2010**, *21*, 075−102.
(45) Rivera-Gil, P.; Jimenez De Aberasturi, D.; Wulf, V.; Pelaz, B.; Del Pino, P.; Zhao, Y.; De La Fuente, J.; Ruiz De Larramendi, I.; Rojo, T.; Liang, X. J.; Parak, W. J. The Challenge to Relate the Physicochemical Properties of Colloidal Nanoparticles to Their Cytotoxicity. *Acc. Chem. Res.* **2012**, *46*, 743−749.
(46) Ehrenberg, M. S.; Friedman, A. E.; Finkelstein, J.N.; Oberdörster, G.; McGrath, J. L. The Influence of Protein Adsorption on Nanoparticle Association with Cultured Endothelial Cells. *Biomaterials* **2009**, *30*, 603−610.

DOI: 10.1021/acsami.5b03873
ACS Appl. Mater. Interfaces 2015, 7, 14983−14991